WPSA-CPR(17) 17641

K Galazka et al.

Multiple impurity seeding for power exhaust management in JT-60SA tokamak with carbon divertor

Preprint of Paper to be submitted for publication in Proceeding of 16th International Workshop on Plasma Edge Theory in Fusion Devices (PET)

This work has been carried out within the framework of the EUROfusion Consortium and has received funding from the Euratom research and training programme 2014-2018 under grant agreement No 633053. The views and opinions expressed herein do not necessarily reflect those of the European Commission.

Article Type

Multiple impurity seeding for power exhaust management in JT-60SA with carbon divertor

K. Gałązka*, I. Ivanova-Stanik, W. Stępniewski, and R. Zagórski

Institute of Plasma Physics and Laser Microfusion, Hery 23, 01-497 Warszawa, Poland

Correspondence: *Corresponding author Email: krzysztof.galazka@ifpilm.pl

Received ? ? 20??; Revised ? ? 20??; Accepted ? ? 20??

Summary

In this work the scenario #2 for the JT-60SA with a carbon divertor configuration is analyzed by using the core-edge integrated COREDIV code. A combined seeding with two impurities, high and low atomic number, is proposed for controlling the core and the scrape-off layer radiation and limiting the total power delivered to the divertor plate. As a proof-of-principle tungsten and argon seeding is investigated due to successful results reported for the same scenario with W divertor. Replacing non-recycling W by recycling Xe shows the influence of the recycling coefficient on the final solution. Also the location of the puffing nozzle was found to be a crucial factor for the final result.

Keywords: JT-60SA, impurity seeding, integrated modelling, COREDIV

1 Introduction

JT-60SA is a superconducting tokamak which aims to support the thermonuclear fusion research on its way towards realization of energy production in DEMO reactor. In the initial phase the JT-60SA a will be equipped with a carbon divertor. Therefore, controlling the conditions at the target is important due to physical and chemical sputtering of C impurity, which leads to strong plasma dilution. The extensive effort of both EU and Japan contributors is to find a suitable operational window for each scenario proposed in the Research Plan [2]. Especially scenario# 2 is one of the most difficult in terms of power control (heating and dissipation).

It is characterized by relatively low average electron density ($\langle n_e \rangle = 5.6 \cdot 10^{19} m^{-3}$) and maximum available applied heating power ($P_{aux} = 41MW$) [2]. The other key parameters are the plasma current $I_p = 5.5$ MA, magnetic field on torus axis $B_T = 2.25$ T and the confinement factor according to IPB98(y,2) scaling law $H_{98(y,2)} = 1.3$. One of the main consequences of these assumptions is high power delivered to the SOL and subsequently to the target plate, which is intolerable for a steady state operation. Our previous calculations performed with core-edge integrated

COREDIV code show that for carbon target the seeding of impurities like N, Ne, Ar and even Kr does not provide enough radiative cooling to mitigate the heat flux delivered to the target plate [6]. It makes the possibility of operating in steady state with low carbon concentrations questionable. The proposed solution was to increase $\langle n_e \rangle$ to values similar to scenario #3, which does not experience such difficulties due to lower auxiliary heating power. On the other hand, when the same scenario is analyzed but with a tungsten divertor, there seem to be at least few kinds of seeded impurities for which solutions are acceptable in terms of target electron temperature and power delivered to the divertor plate [1]. The reason was the intrinsic tungsten impurity, which provides the main radiation channel in the central plasma. Up to some extent in this way the presence of intrinsic W in the core plasma is beneficial as it limits the heat flux delivered to the SOL and to the target without strong dilution of the fuel. The aim of this work is to design an impurity mix for C divertor which would act in the same way as W in the scenario#2 with W divertor.

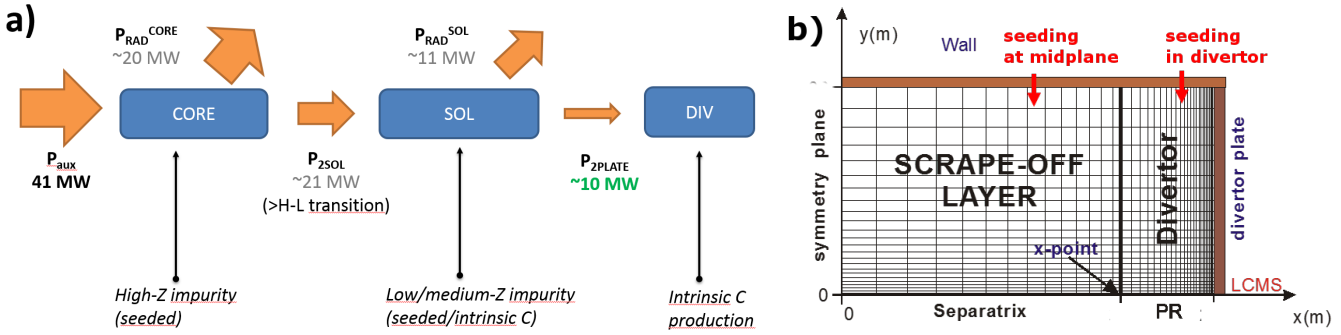

Figure 1: a) The design of energy flow in scenario #2 of JT-60SA for carbon divertor. The intentional radiation levels are provided by impurities. b) The 2D slab SOL geometry used in COREDIV and the locations of puffing valves.

Our strategy was to try to apply high Z and medium Z impurity simultaneously, additionally to the intrinsic C production. This idea is graphically described in Figure 1. The intended radiation fraction should be at least 70%. Due to currently available model, the heavy impurity - W is introduced to the plasma as a gas puff. For tungsten and other metals using it as a gas puff is not practical, but one might consider it as a way to simulate pellet/shattered pellet injection process. Of course the spatial distribution of the seeded impurity source is still very different for puffing and pellet injection but the general qualitative conclusions should give a hint on the predicted behavior. To demonstrate control over the power radiated from the core and the SOL for selected cases also additional Ar seeding is performed. The second impurity, if present, is always puffed in the divertor.

In COREDIV the neutrals in the SOL region are described by a simplified analytical model based on a diffusive behavior. The hydrogen neutrals source situated in the vicinity of the target plate is controlled by self-adjustable recycling coefficient (to keep the prescribed average electron density). In the case of intrinsic impurity the source is mainly the sputtering process at the target and a fixed recycling coefficient R. The recycling coefficient is defined as

$R = {}^{(\Psi_{div} - \Psi_{in})}/_{\Psi_{div}}$, where Ψ_{in} is the total impurity ions flux into the SOL and Ψ_{div} is the total impurity ion flux to the divertor plate. In the case of the seeded impurity in addition to its recycling coefficient giving rise to a source near the target plate, the external source is defined by a 2D profile function, peaked at the location of the nozzle at the wall, normalized to keep the prescribed total seeding rate. Thus the source of plasma ions (main plasma and impurities, all ionization stages) is then defined by intensity of atomic processes: charge-exchange, ionization and recombination, in accordance to local conditions (rate coefficients, neutral density, electron temperature, electron and ion densities and so on). Summing up, main plasma and impurities have sources located near the target and defined by recycling or sputtering coefficient, but seeded impurities have additional source situated at a defined spot on the wall (see Fig. 1). The model takes into account the important processes and enables fast computation while sacrificing the behavior of neutral particles and the description of rich details of plasma-wall interaction.

As a next step Xe is applied instead of W to investigate a situation closer to real-life. This case serves as a demonstration of how gas recycling properties and location of the puffing nozzle can lead to a dramatically different scenario development. Two locations of the puffing nozzle are investigated as shown in Figure 1 b): in the divertor (90% of the distance along the wall between the stagnation point and the target) and around the midplane (50% of the distance along the wall between the stagnation point and the target). Recycling coefficients of Xe and W are fixed to 0.925 and 0.25, respectively. But to demonstrate the influence of the recycling properties of a gas on its behavior and resulting solution a scan of the R_{Xe} for Xe is performed when it is varied from the original value to the one used for tungsten (0.25). All the calculations were done by using COREDIV code.

The COREDIV code consists of 1D model of the central plasma and 2D model of the SOL region interconnected at the separatrix by appropriate boundary conditions. As its main features of are described elsewhere ([1, 3–5, 7]). The adjustable parameter anomalous diffusion coefficient in the SOL is 0.5 m^2/s and the electron density at the separatrix is equal to 40% of the average electron density in the core. The additional expressions for transport coefficients and energy confinement time are given in our previous publication [6].

2 Simulation results

2.1 Tungsten seeding

To mimic the mentioned radiation channel connected with tungsten impurity in the scenario #2 of JT-60SA with W divertor gas puff of tungsten for the setup with a carbon divertor was applied. The position of the gas puff nozzle was fixed to the divertor or to the midplane, according to Figure 1 b). It must be emphasized that for the midplane position far more gas was able to penetrate to the central plasma than for the puffing nozzle location in divertor.

It is the main reason of why the midplane position is considered. In Figure 2 the main plasma parameters vs. W concentration (c_W) are presented.

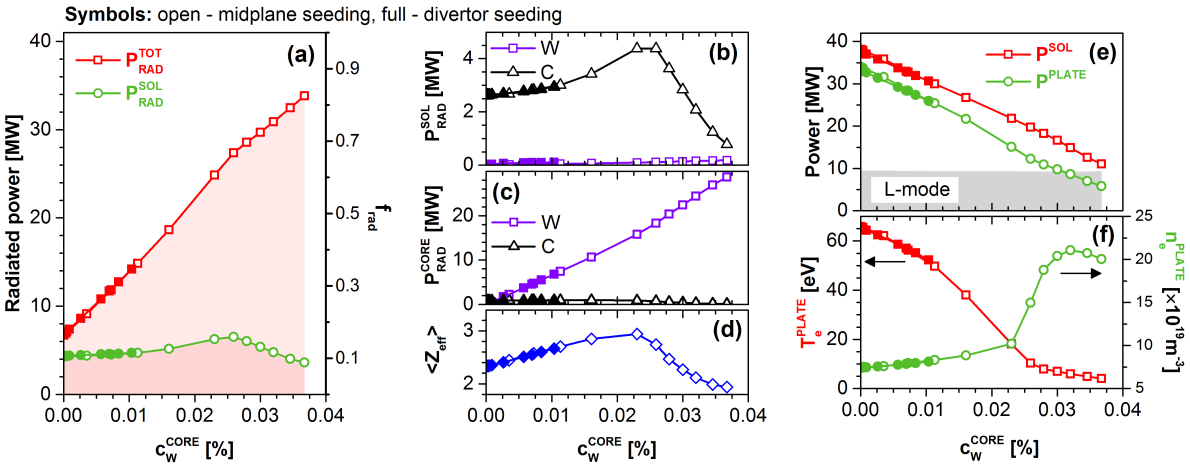

Figure 2: Overview of the results for scenario #2 as a function of tungsten concentration: a) radiation power b) radiation in the SOL for impurities, c) radiation in the core for impurities, d) average effective charge, e) power delivered to the SOL and to the target plate (the gray area denotes operation under the L-H transition limit), f) electron temperature (left scale) and density (right scale) at the target.

It can be observed that in the core tungsten is the main radiation channel in the core and carbon is the dominant impurity in the SOL. Radiative heat losses due to W radiation reach almost 29 MW in the central plasma. A clear onset of detachment is visible at $c_W^{CORE} \approx 2.3 \cdot 10^{-4}$, indicated by the arrow. In the more pronounced detachment phase the production of carbon impurity (by sputtering) is much lower what corresponds to a decline of C radiation in the SOL, as well as in the central plasma. One can also notice that the average effective charge is controlled by C concentration. The maximum reached value of Z_{eff} is 2.9, which diminishes subsequently to ~ 1.9. In this way the possibility of reconstruction of the same heavy impurity radiation channel as in scenario #3 is confirmed for scenario #2 [1]. However, it must be emphasized that the crucial parameter is the position where gas puff is applied. The full points denoting gas puff in the divertor end at much lower c_W^{CORE} than the open ones for gas puff position at the midplane. It is a consequence of different plasma environment at the puffing nozzle, leading to very different injected impurity behavior. This problem will be wider examined in the case of Xe seeding.

Figure 2 confirms that with increasing c_W^{CORE} the power delivered to the SOL is efficiently limited from ~ 38 MW to ~ 11 MW. The power delivered to the target plate is limited as well, to about 6 MW for the best case. The onset and progress of detachment can be observed in Figure 2 b) as a significant increase in the electron density at the divertor plate and limiting of the corresponding electron temperature to the range 10 - 4 eV.

These beneficial conditions in the divertor can be achieved by seeding of heavy, tungsten-like impurity. On the other hand, the power delivered to the SOL for the highest W seeding is very close to the L-H transition limit (gray

area in the Figure 2 a). Therefore, to keep the power to the SOL above the L-H transition a constant background level of W puffing is selected and a scan with Ar impurity is performed. It must be emphasized that this W puffing rate is achieved only for the midplane gas puff position.

2.2 Multiple impurity seeding (W + Ar)

After the successful application of W puff an additional puff of Ar was added for the fixed background level of $\Gamma_W = 5 \cdot 10^{19} s^{-1}$, which corresponds to $c_W = 1.6 \cdot 10^{-4}$. The results are presented in Figure 3. The radiation fraction reaches at most 70%. In the conditions set by the background tungsten seeding level Ar is found to radiate (and reside) in the SOL as well as in the core plasma. Due to that fact Z_{eff} stays at the level of about 3. The biggest benefit can be observed in Figure 3 e). With combined W and Ar seeding for the highest Ar seeding rate the detachment can be approached with almost unchanged power delivered to the SOL (22 - 19 MW). The power delivered to the target falls almost to 10.7 MW, n_e^{PLATE} and T_e^{PLATE} reach $17 \cdot 10^{19} m^{-3}$ and 8 eV, respectively, similar values as with pure W seeding before. It can be foreseen that with using an impurity with lower atomic number than Ar the radiation in the SOL should be increased and carbon, which radiation is already declining with Ar gas puff, should be completely replaced (compare Figure 3 in reference [6]).

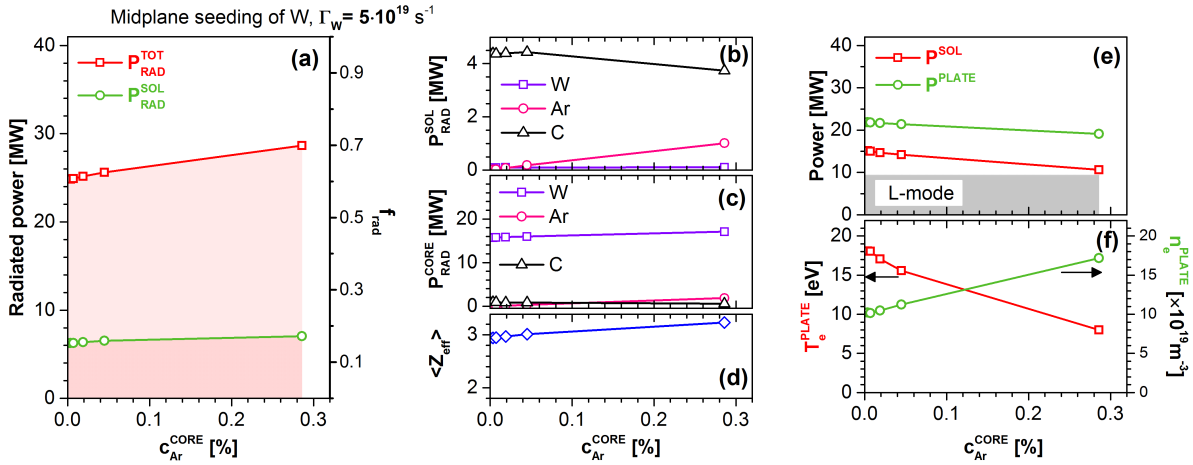

Figure 3: Overview of the results for scenario #2 as a function of argon concentration for a constant W seeding rate $\Gamma_W = 5 \cdot 10^{19}$: a) radiation power b) radiation in the SOL for impurities, c) radiation in the core for impurities, d) average effective charge, e) power delivered to the SOL and to the target plate (the gray area denotes operation under the L-H transition limit), f) electron temperature (left scale) and density (right scale) at the target.

2.3 Multipe impurity seeding: Xe + Ar

In the next step a different seeding gas more practical to use instead of tungsten was applied. Basing on our previous experience with this scenario Xe was chosen for its high mass and atomic number. As previously for W, Ar is chosen

as the second impurity. At first a scan with Xe seeding is performed. Only results for seeding in the divertor are presented (Figure 4 a), b), c) and d)). Subsequently, Ar was added for a selected Xe background level. Several base Xe seeding rates were and investigated but as the observations lead to similar conclusions, only $\Gamma = 4 \cdot 10^{19} \mathrm{s}^{-1}$ is presented (Figure 4 e), f), g) and h) for the Xe seeding in the divertor and Figure 4 i), j), k) and l) for the Xe seeding at the midplane).

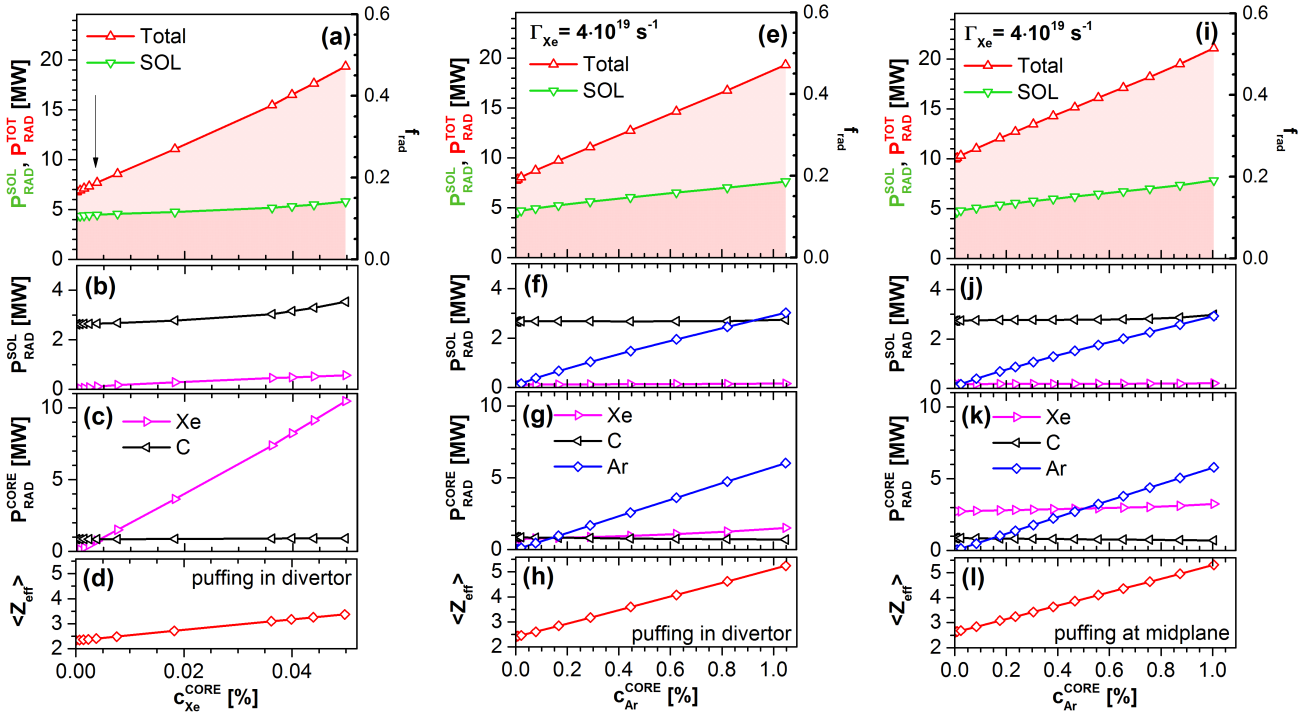

Figure 4: Overview of the results for scenario #2 for Xe seeding (a, b, c and d), Ar seeding with constant Xe background puffed in the divertor (e, f, g and h) and at the midplane (i, j, k and l) as a function of tungsten concentration. a), e) and i) radiation power, b), f) and j) impurity radiation in the SOL, c), g) and k) impurity radiation in the central plasma, d), h) and l) average effective charge. Ar seeding is always performed in the divertor.

All the results show that it is not possible to get a stationary solution with f_{RAD} values higher than 50-55%. Xe radiation in the core (about 10 MW) is too small to provide enough radiative cooling (see Figure 4 c)). High level of C radiation in the SOL for each case (Figure 4 b, f and j) evidences that the C production is not suppressed, therefore conditions are far from detached. The c_C varies from 3.6 to 4.7% for all cases. In the case with Ar seeding Ar helps to radiate some fraction of power in the SOL as well as in the central plasma, but it is still not enough to get a significant f_{RAD} levels. Also much higher Z_{eff} are observed when Ar seeding is applied (in the range 2.5 - 5.5 compared to the range 2 - 3.5 without Ar seeding).

An interesting observation is that Xe radiation levels in the core (connected to Xe concentrations) increase when Ar is added despite a constant level of Xe background seeding. This fact is connected with increasing temperature gradients when Ar radiation in the SOL cools down the divertor plasma. The thermal force is stronger for steeper

T gradients and pulls Xe ions into the core. The increase of the Xe core radiation is significant (from 0.75 MW to 1.5 MW for seeding in divertor and from 2.7 MW to 3.3 MW for seeding at midplane), but does not change the final solution much. The biggest difference is that in the case when Ar seeding is applied for the Xe seeding in the midplane the Xe radiation in the central plasma (and its concentration) is approximately 2 MW higher than when Ar scan is performed for Xe seeding in the divertor. This indicates that for seeding at the midplane Xe is more efficiently delivered to the central plasma than when the seeding nozzle position is in the divertor due to different plasma conditions. However, in the this case the influence of the mentioned effects on the radiation fraction is not big (radiation fraction 0.47 for seeding in divertor compared to 51.5 for seeding at midplane).

It must be also mentioned that an attempt to further increase the radiation fraction by increasing Xe seeding from the $\Gamma_{\mathrm{Xe}} = 4 \cdot 10^{19}\mathrm{s}^{-1}$ level but a self-consistient, steady-state solution was found only up to $\Gamma_{\mathrm{Xe}} = 5.5 \cdot 10^{19}\mathrm{s}^{-1}$. It was characterized by $f_{\mathrm{RAD}} \simeq 0.5$, $\mathrm{P}_{\mathrm{RAD}}^{\mathrm{CORE,Xe}} = 5.3$ MW and $\mathrm{P}_{\mathrm{RAD}}^{\mathrm{CORE,Ar}} = 3.6$ MW. Altogether, $\mathrm{P}_{\mathrm{RAD}}^{\mathrm{TOT}} = 19.7$ MW, similarly as for the previously discussed cases. Summarizing, all the efforts to have similar radiation fraction as with tungsten seeding failed, including change of the gas puff location to the midplane.

2.4 Modification of the recycling coefficient of Xe

As moving the gas puff position to the midplane did not help to deliver more Xe to the central plasma and obtain a radiation fraction higher than 0.7 another parameter was investigated. In contrary to W which is a non-recycling element with $\mathrm{R_W} = 0.25$, Xe as a noble gas is a recycling element and normally in COREDIV its recycling coefficient is set to $\mathrm{R_{Xe}} = 0.925$. To check whether this property prevents Xe to behave similarly to W the recycling of Xe was changed to the value used previously for W and for the results shown in Figure 5 $\mathrm{R_{Xe}} = 0.25$.

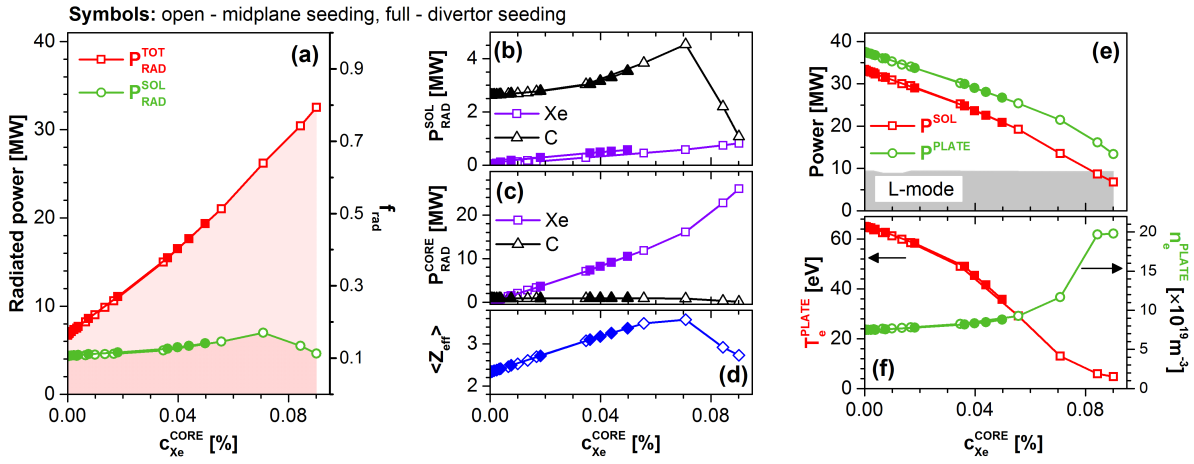

Figure 5: Overview of the results for scenario #2 as a function of Xenon concentration: a) radiation power b) radiation in the SOL for impurities, c) radiation in the core for impurities, d) average effective charge, e) power delivered to the SOL and to the target plate (the gray area denotes operation under the L-H transition limit), f) electron temperature (left scale) and density (right scale) at the target.

For a better comparison, in Figure 5 also the data from Figure 4 a), b), c) and d) is displayed as full symbols. One can immediately see that by changing the recycling coefficient Xe gained similar properties as tungsten before. More Xe can be delivered to the central plasma and the range of c_{Xe} for which a stable solution is obtained is extended. The onset of detachment is visible close to $c_{Xe}^{CORE} = 0.07$ %, indicated by the decline of C radiation and Z_{eff}. This decline corresponds to a sharp step of the electron density at the target and fall of thr electron temperature at the target from 13 eV to 4.7 eV (see Figure 5 b). Simultaneously the power delivered to the SOL stays above the L-H limit and the power reaching the target is below 10 MW (see Figure 5 a)). The results for maximum Xe seeding level are comparable to the ones obtained for W when the gas puff position is at the midplane and their recycling properties are the same.

The source of Xe atoms due to recycling in the divertor is affected by the R_{Xe} setting. In Figure 6 a) and c) a 2-D map of Xe atoms distribution in the SOL is presented. The selection is made for the highest achieved Xe gas puff levels. It is clearly visible that in the case with high recycling the dominant Xe source is not the gas puff but the recirculating Xe near the target plate. The position of the gas puff nozzle is of secondary importance. Xe gas is not transported to the core plasma efficiently enough to limit the downstream flux of energy and momentum (see the plasma velocity map below) and the conditions remain attached. On the other hand, for $R_{Xe} = 0.25$ the relative importance of the recirculating Xe in the divertor region is much smaller (Figure 6 c)). The gas puff level is not limited by the intensity of the source in the divertor and much higher Γ_{Xe} value can be reached. Due to the nozzle location at the midplane (lower plasma velocities) more Xe can be delivered to the core. There, due to the Xe line radiation it actually acts as a heat dissipation channel. As an effect the energy delivered to the SOL is lower, which results in significantly lower plasma velocities (Figure 6 d)) what is beneficial for transport of Xe ions to the plasma core as well as achieving detachment. One can se a significant difference of velocity profile along the target (Figures 6 b) and d), next to vertical scale) demonstrating a dramatic decrease of velocity at the strike point and a shift of velocity maximum towards the wall, characteristic for semi-detached conditions.

3 Discussion and conclusions

The idea of power exhaust management by radiation of seeded impurities for scenario #2 is successfully demonstrated for a combination of tungsten and argon seeding. An important factor is the location of the puffing nozzle. Figure 2 demonstrates that when the location is at the midplane the central plasma is much more accessible for the introduced impurity. As a result, more gas can be delivered to the core and act as an additional radiation channel. It is beneficial for this particular scenario, which suffers from the lack of enough core radiation and too high power delivered to the target. This can be a valuable information for the preparation of experiment, not only concerning the gas puff but also pellet/shattered pellet injection. Although the results for W and Ar seeding indicate that management of the

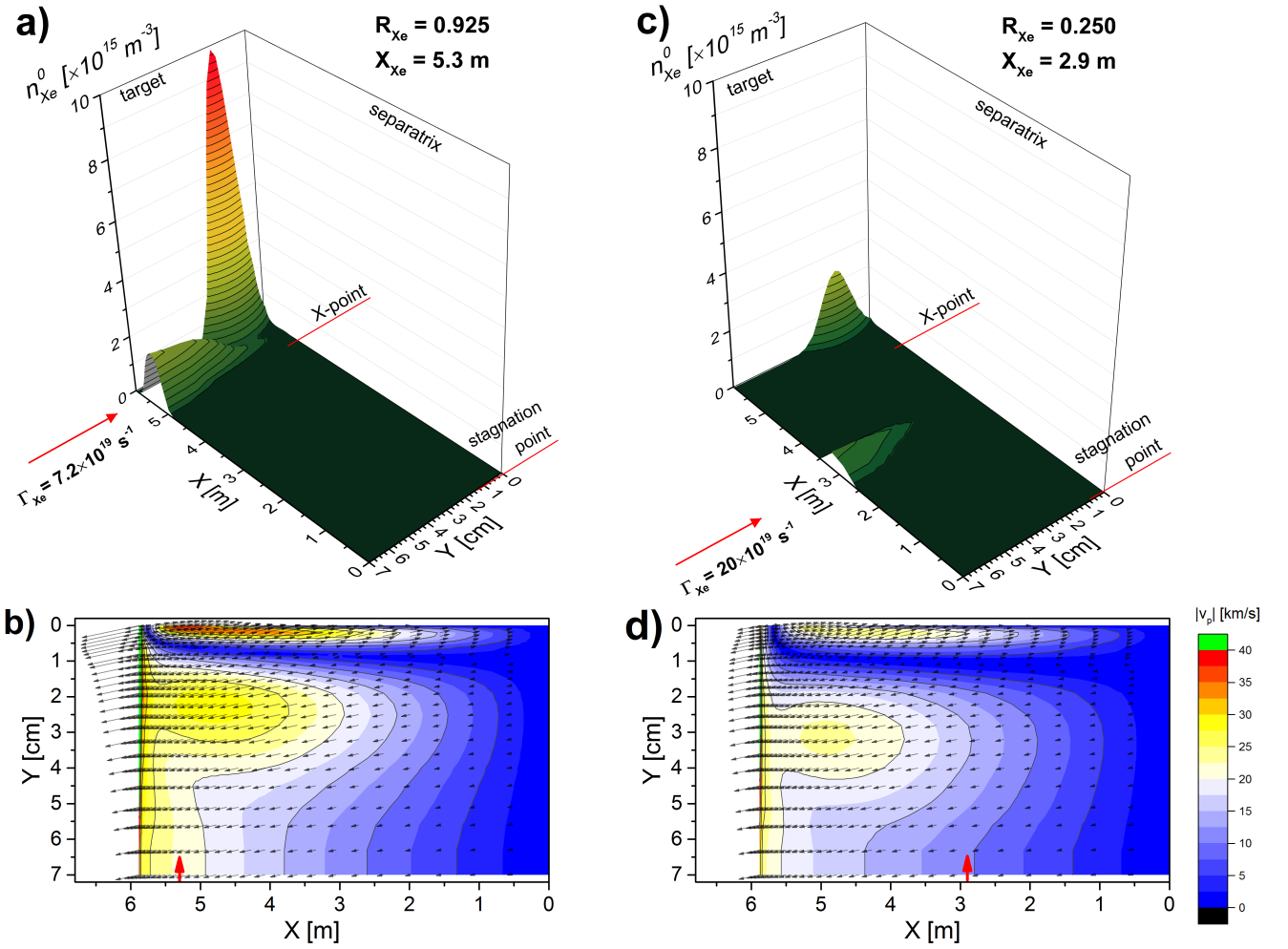

Figure 6: The distribution of Xe atoms in the SOL: a) for the case of Xe seeding in the divertor and original recycling coefficient, c) for the case of Xe seeding at the midplane and modified recycling coefficient. Below each part a corresponding velocity map is located (b and d). Red arrow indicates the position of Xe gas puff nozzle.

heat dissipation through W and Ar line radiation is possible the same idea for Xe and Ar seeding combination is not readily repeatable. The investigations show that beside the gas puff location the key parameter is the recycling of the gas used (R_W=0.250 is non-recycling and R_{Xe}=0.925 is a recycling gas). Only by an artificial change of Xe recycling coefficient to the one of tungsten the previous result for W seeding could be recovered. A comparison for non-recycling and recycling Xe shows that the recycling gas tends to accumulate near the target plate, what makes the location of puffing source a marginal factor. This effect also limits the maximum applied gas puff to moderate values, not allowing for enough Xe to be transported to the central plasma. In the case of the non-recycling gas the nozzle location affects deeply the results. The midplane puffing of a non-recycling gas leads to a higher impurity concentration and radiation in the central plasma, resulting in larger dissipated power and milder conditions in the SOL, what can be observed at for instance SOL plasma velocity maps. The results can be a valuable hint for the power exhaust problem when selecting a seeding gas, which is desired to radiate in the core. However, one should take into account that beside the recycling properties the elements have also other properties which can be of importance

for the final result, like atomic number or ionization energy. For a suitable candidate a similar simulation would be required. Nevertheless, this study helps to better understand and control the impurity behavior.

Acknowledgments

This work has been carried out within the framework of the EUROfusion Consortium and has received funding from the Euratom research and training programme 2014-2018 under grant agreement No 633053. The views and opinions expressed herein do not necessarily reflect those of the European Commission. This scientific work was partly supported by Polish Ministry of Science and Higher Education within the framework of the scientific financial resources in the year 2017 allocated for the realization of the international co-financed project.

References

[1] K. Gałązka, I. Ivanova-Stanik, W. Stępniewski, R. Zagórski, R. Neu, M. Romanelli, T. Nakano, *Plasma Physics and Controlled Fusion* **2017**, *59(4)*, 045011.

[2] JT–60SA Research Unit, JT–60SA Research plan – research objectives and strategy, Version 3.3, **2016**

[3] R. Stankiewicz, R. Zagórski, *Czechoslovak Journal of Physics* **2002**, *52*, D32–D37.

[4] R. Stankiewicz, R. Zagórski, *Journal of Nuclear Materials* **2005**, *337-339*, 191–195. PSI-16.

[5] G. Telesca, R. Zagórski, S. Brezinsek, W. Fundamenski, C. Giroud, G. Maddison, M. O. Mullane, J. Rapp, M. Stamp, G. V. Oost, JET EFDA contributors, *Plasma Physics and Controlled Fusion* **2011**, *53(11)*, 115002.

[6] R. Zagórski, G. Giruzzi, K. Gałązka, I. Ivanova-Stanik, M. Romanelli, W. Stępniewski, *Nuclear Fusion* **2016**, *56(1)*, 016018.

[7] R. Zagórski, G. Telesca, G. Arnoux, M. Beurskens, W. Fundamenski, K. McCormick, *Journal of Nuclear Materials* **2009**, *390-391*, 404–407.